



# I.FAST

Innovation Fostering in Accelerator Science and Technology  
Horizon 2020 Research Infrastructures GA n° 101004730

## DELIVERABLE REPORT

# First Engineering design of HTS demonstrator

### DELIVERABLE: D8.3

---

<b>Document identifier:</b>	IFAST-D8.3
<b>Due date of deliverable:</b>	End of the Month 18 (October 2022)
<b>Justification for delay:</b>	Delivered on Month 24 (lack of personnel)
<b>Report release date:</b>	30/04/2023
<b>Work package:</b>	WP8:Innovative Superconducting Magnets
<b>Lead beneficiary:</b>	INFN
<b>Document status:</b>	Final

---

### ABSTRACT

The following report presents the first engineering design study of the CCT magnet demonstrator based on HTS. The report highlights the geometry, quench protection and AC-losses of the coil. The conductor geometry with the equations and the geometry are presented in first section. The magnetic design with the focus on the field quality is described in the second section. The materials and manufacturing concept are shown in the fourth section. The fifth section is dedicated to the thermal design aspect. A protection study based on a two-dimensional adiabatic model is reported in the sixth section. In the last section, the AC losses are calculated in order to determine the number of tapes in the conductor.

ARIES Consortium, 2023

For more information on IFAST, its partners and contributors please see <https://ifast-project.eu/>

This project has received funding from the European Union's Horizon 2020 Research and Innovation programme under Grant Agreement No 101004730. IFAST began in May 2021 and will run for 4 years.

### Delivery Slip

	Name	Partner	Date
<b>Authored by</b>	E. De Matteis, S. Sorti	INFN	07/04/2023
<b>Edited by</b>	E. De Matteis, S. Sorti	INFN	07/04/2023
<b>Reviewed by</b>	T. Lecrevisse	CEA	07/04/2023
<b>Approved by</b>	M. Vretenar [on behalf of Steering Committee]		30/04/2023



---

## TABLE OF CONTENTS

<b>1. INTRODUCTION.....</b>	<b>5</b>
<b>2. CONDUCTOR GEOMETRY.....</b>	<b>6</b>
1.1 FRENET-SERRET FRAME .....	6
1.2 COIL GEOMETRY.....	7
<b>3. MAGNETIC DESIGN.....</b>	<b>10</b>
3.1 GEOMETRIC FIELD QUALITY.....	10
<b>4. MATERIALS AND MANUFACTURING CONCEPT.....</b>	<b>12</b>
<b>5. THERMAL DESIGN.....</b>	<b>13</b>
<b>6. QUENCH PROTECTION .....</b>	<b>14</b>
<b>7. AC LOSSES AND DYNAMIC FIELD QUALITY.....</b>	<b>24</b>
<b>8. CONCLUSIONS .....</b>	<b>27</b>

## ***Executive summary***

*The engineering design report presented represents a first study of the Canted Cosine Theta (CCT) demonstrator based on High Temperature Superconductor (HTS) from the conductor, magnetic, manufacturing, thermal, protection and power losses point of view.*

*The HTS demonstrator magnet was designed with a CCT layout because the flat REBCO HTS tapes cannot undergo hard-way bending. To avoid or minimize such bending, the Frenet-Serret frame was used in the CCT equations.*

*This report proposes two geometries for the 4 T magnet demonstrator based on the CCT layout. The first geometry uses a cable with two 4mm-wide tapes and has 23 cables in each slot of the two formers, operating at 970 A. The second geometry uses a cable with four 4mm-wide tapes and has 11 cables in each slot of the two formers, operating at 1990 A.*

*To improve current sharing, the HTS and copper stabilizer tapes in the cable of the coil should be soldered together, but due to bending shear stress, they must be wound separately on the former before soldering.*

*Adiabatic quench analysis showed that for a quench detection voltage threshold of 0.3 V, a protection delay of 20 ms and a protection voltage of 500 V using a varistor unit, the required thickness of copper stabilizer tapes is 350  $\mu\text{m}$  and 700  $\mu\text{m}$  for the two-tape and four-tape designs, respectively, to keep peak temperature within an acceptable 250 K.*

*Geometric field quality can be achieved by controlling the Fourier series coefficients that describe the coil's radius.*

*The AC-losses during operating for both designs are on average 50 W. This is compatible with a conduction cooling system at 20 K.*

---

## 1. Introduction

---

The WP8 Innovative Superconducting Magnets of the H2020 – EU project IFAST has the scope to form a permanent European Strategy Group, open to worldwide partners, to discuss the European strategy for HTS magnets for accelerators, and to improve Industry involvement in this technology. The main technological goal is to explore Canted Cosine Theta (CCT) magnet with HTS superconductor, preceded by a combined function CCT based on LTS involving the industries that want to learn about the CCT magnets. The baseline magnet parameters are fixed in sharing with the other EU program, HITRI*plus*, oriented to study hadron therapy magnets. The geometry of the two demonstrators is straight for matter of simplicity.

The Task 8.3 (Preliminary Engineering design of HTS Canted Cosine Theta (CCT)) should (i) define the best option for the magnet structure and magnetic design at conceptual level for the HTS CCT scaled demonstrator, (ii) provide technological tests (small coils) and a preliminary engineering design of a scaled prototype, and (iii) procure and qualify the HTS superconductor for the construction of the demonstrator. The task should also consider how the medical-applications design can be used, with minor modifications, for nuclear and high energy physics applications, in synchrotrons or beamlines for experimental areas. The aim of the CCT HTS demonstrator is to reduce dimensions and cost of synchrotrons and gantries for research and for cancer therapy, constructing the prototypes with advanced components.

This report represents the first engineering design of the CCT based on HTS, investigating the geometry, quench protection and AC-losses of the coil. First, the equations used to describe the coil geometry and the design of the coil itself are described in Section 2. The magnetic design of the demonstrator is reported in the Section 3. This section discusses also how to avoid hard-way bending of the conductor, while still guaranteeing an accelerators-level field quality. Some considerations on the manufacturing of such a coil are provided in Section 4. The coil thermal margin used for determining the number of conductors or sub-layers in a CCT slot is shown in Section 5. The quantity of copper used in the design was calculated using a two-dimensional adiabatic quench model, which is described in Section 6. The AC-losses, important for determining the number of tapes in the conductor or sub-layer, are calculated in Section 7. Finally, the conclusion is drawn in Section 8.

## 2. Conductor Geometry

### 1.1 FRENET-SERRET FRAME

The coil geometry of a CCT magnet can be described using a space-curve  $\overline{R(\theta)}$ , located at the inner radius of the CCT, running along  $\theta$  on the interval  $\pi n_{t1}$  to  $\pi n_{t2}$ , where  $n_{t1}$  and  $n_{t2}$  specify the turn range. The equation describing the space-curve is given as

$$\overline{R(\theta)} = \rho(\theta) \cos(\theta) \vec{e}_x + \rho(\theta) \sin(\theta) \vec{e}_y + \left( A_i(\theta) \sin(n\theta) + \frac{\omega}{2\pi} \right) \vec{e}_z \quad (1)$$

where  $\rho(\theta)$  is the radius of the coil, which can be a function of theta for non-round apertures (this is used later in this work to achieve good field quality),  $n$  is the number of poles, in the case of a dipole equal to 1,  $e_x$ ,  $e_y$  and  $e_z$  are the unit vectors in the x, y and z directions, respectively. The amplitude of the oscillations in the z-direction  $A_i$  is calculated as

$$A_i(\theta) = \frac{\rho(\theta) \tan(\alpha_i)}{n_i} \quad (2)$$

where  $\alpha_i$  is the skew angle. Note that the amplitude becomes dependent on  $\theta$  for non-round apertures. The derivatives of the space curve are given as  $\vec{V}$  (velocity),  $\vec{A}$  (acceleration) and  $\vec{J}$  (jerk), which are calculated analytically. To get the orientation of the tapes around the space curve the Frenet-Serret equations are used. First, we calculate the torsion  $\tau$  and curvature (in the normal direction)  $\kappa$  as

$$\tau = \frac{(\vec{V} \times \vec{A}) \cdot \vec{J}}{|\vec{V} \times \vec{A}|^2}, \quad \kappa = \frac{|\vec{V} \times \vec{A}|}{|\vec{V}|^3} \quad (3)$$

The frame describing the orientation of the conductor along the length of the space curve then becomes

$$\vec{L} = \frac{\vec{V}}{|\vec{V}|}, \quad \vec{B} = \frac{\vec{V} \times \vec{A}}{|\vec{V} \times \vec{A}|}, \quad \vec{D} = \frac{\sqrt{1 + \frac{\tau}{\kappa}(\tau \vec{L} + \kappa \vec{B})}}{|\tau \vec{L} + \kappa \vec{B}|}, \quad \vec{N} = \vec{B} \times \vec{D} \quad (4)$$

where  $\vec{L}$  are the longitudinal unit vectors,  $\vec{B}$  the bi-normal vectors,  $\vec{D}$  the Darboux vectors and  $\vec{N}$  are the normal vectors. Using these vectors, the space-curve can be shifted in the N and D directions to form the edges of each cable or the nodes of the mesh for example. For further information interested readers are referred to Stephan Russenschuck's book on Accelerator Magnets [1].

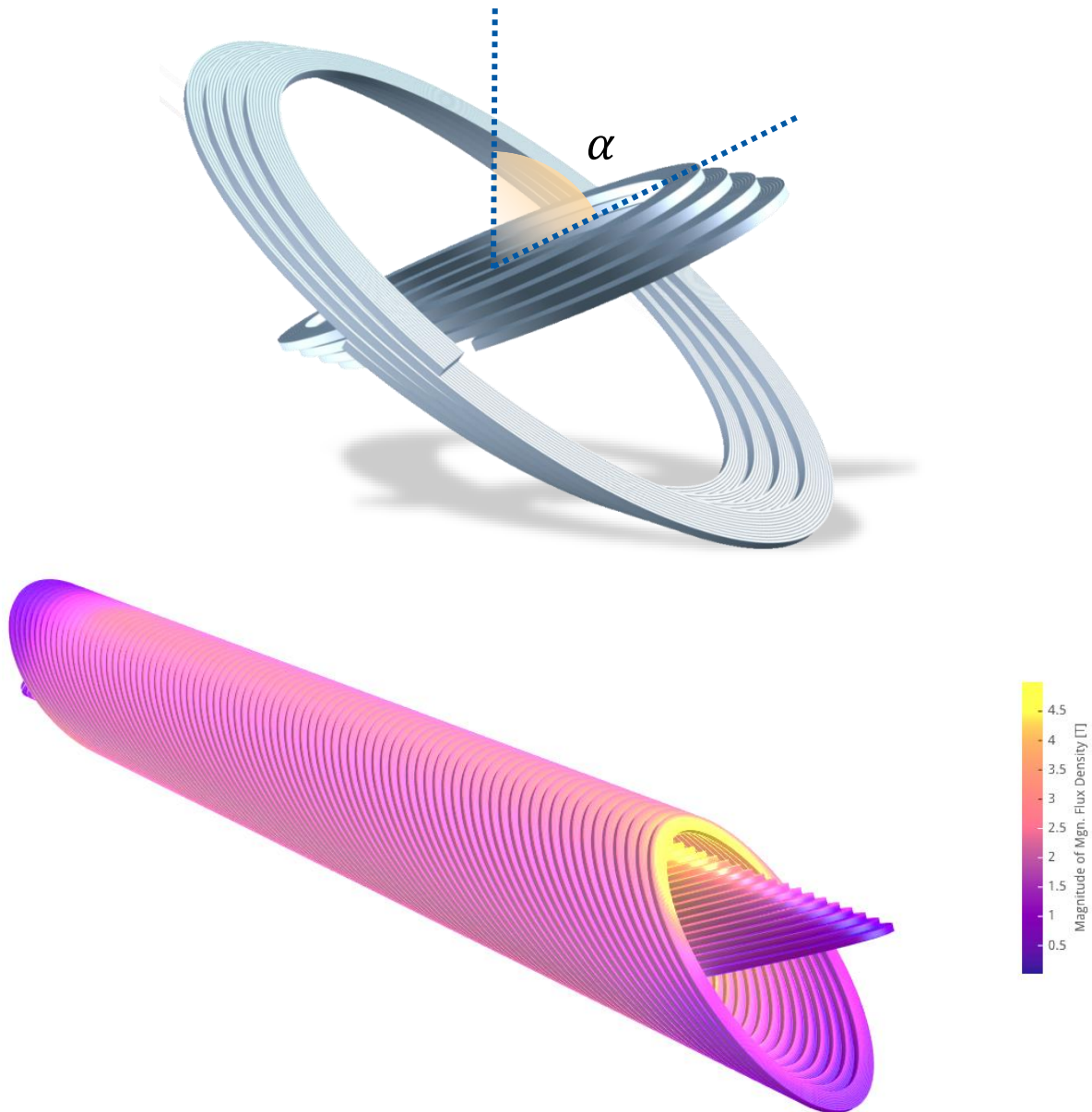


Fig. 1 A rendering showing a few turns of the winding geometry of the HTS CCT coil (top), and the flux density on the conductor (bottom) modelled using RAT [2].

## 1.2 COIL GEOMETRY

Typically, CCT coils have a skew winding angle of  $\alpha=60^\circ$  (measured as shown in Figure 1), which is what is chosen for the inner layer. For the outer layer, a skew angle of  $50^\circ$  is instead taken. This makes the coil-end approximately the same length for both layers and, as far as the winding pitch  $\omega$  is the same, the axial field (solenoidal) component is cancelled inside magnet aperture. Due to the soft-way bending requirement, the tapes of the CCT magnet lie flat (i.e., with the width direction perpendicular to the groove) on the coil former on the mid-plane.

This has the disadvantage of placing a minimal winding pitch  $\omega$  length between the turns, given as

$$\omega = \frac{w_{tape} + w_{rib}}{\cos(\alpha)} \quad (5)$$

where  $w_{tape}$  is the width of the tape and  $w_{rib}$  is the thickness of the rib between the cables. A pitch  $\omega$  of 10 mm is chosen, which leaves a rib thickness  $w_{rib}$  of 0.98 mm for the first layer and 2.4 mm for the second layer.

In order to reach the required field of 4 T it is needed to have about 22 kA total per conductor, per groove, in each former. Since this is well over the 2 kA limit that we take as upper limit to avoid excessive heat load from the current leads. It is highly recommended that a cable consists of multiple tapes in parallel to mitigate possible defects in the tape. For example, in case of a defect, a cable containing 2 tapes can still carry 50% of the original current and a cable with 4 tapes 75% of its original current. For the sake of calculations, we adopt Fujikura FESC-SCH04 [6], which has a 660 A at 20 K under 5 T transverse field (see Table 1). In order to stay above a temperature margin of 10 K (see Sections 5 and 6), the two-tapes option requires 23 cables per former, carrying 970 A. For the four-tape option, we need 11 cables, each carrying 1990 A.

In addition to the copper coating of the HTS tapes, extra copper stabilizer copper (bulk or in tapes) will be needed to share the current during discharge around the normal zone in the event of a quench. It is recommended to orient the so-called type-0 pairs together. This means that the superconductor layers are facing one another. For the four-tapes cable, different combination of tapes orientation should be further investigated. A large layer of located on the superconductor side is not recommended due to the copper potentially applying a shear force on HTS when it deforms under Lorentz forces.

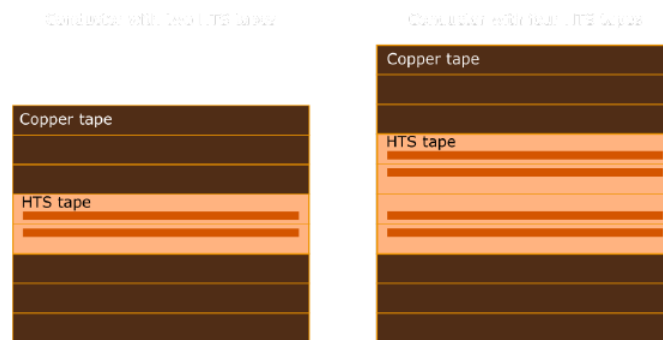


Figure 2. Schematic drawing of the conductor design with two HTS tapes on the left and four HTS tapes on the right. The number and the width of copper tapes that sandwich the HTS tapes should be based on the maximum hot-spot temperature after a quench event.

To maximize the current sharing between the HTS and the stabilizer copper tapes, the copper tapes should be soldered to the HTS and to themselves, or at least in good electrical contact. This needs to be done inside the cable, but shorts between turns must be avoided. However, when such a cable is bent, the tapes on the inside have a shorter path length than the tapes on the outside, which means they need to be able to slide with respect to each other during winding. Since the bending radius is in the order of 50 mm the tapes cannot be soldered together before winding, because that would cause

de-lamination of the HTS tapes. Instead, the tapes should be wound from separate spools and tensioners to accommodate the differential length, then after they are mounted into the slot they need to be soldered together. To achieve this, the following conductor design and winding process are proposed. The conductor will either have two or four HTS tapes, where the HTS sides of the tapes are facing each other in pairs. On both sides of the HTS tapes there will be a stack of copper tapes for stabilisation, see Figure 2. The tapes, both the HTS tapes and the copper tapes, should be soldered together in order to improve current sharing. The winding process is non-trivial and is described in Section 4. Both designs (two and four tapes) are detailed in Table 2.

*Table 1. FESC-SCH04 main characteristics*

Width [mm]	Thickness [mm]	Substrate [ $\mu\text{m}$ ]	Stabilizer [ $\mu\text{m}$ ]	Ic [A] @77K, Self-field	Ic [A] @20K, 5T	Remarks
4	0.11	50	20	$\geq 85$	663	Art. Pin.

*Table 2. Design parameters of the I.FAST CCT for either two (left) or four (right) HTS tapes in parallel.*

Parameter	Two HTS tapes	Four HTS tapes
	Value	Value
Coil length	1 m	
$n_{layers} \times n_{turns}$	$2 \times 85$	
$n_{sub-layers}$	23	11
$\omega$	10 mm	
$a_{0,inner}$	44 mm	
$a_{0,outer}$	64 mm	
$a_4$	0.12 mm	0.09 mm
$a_6$	-0.015 mm	
$\alpha_{inner}$	$60^\circ$	
$\alpha_{outer}$	$50^\circ$	
$w_{tape}$	4.0 mm	
$w_{rib,inner}$	0.98 mm	
$w_{rib,outer}$	2.4 mm	
$T_{op}$	20 K	
$T_{margin}$	10 K	
$I_{op}$	980 A	1990 A
$L$	240 mH	50 mH

### 3. Magnetic Design

#### 3.1 GEOMETRIC FIELD QUALITY

Since the tape is not at a right angle with respect to the former, in contrast to LTS CCT magnets, a field error is introduced. To reduce this field error the radius of the coil can be described using a Fourier series of  $\theta$  as

$$\rho(\theta) = \sum_{n=0}^{\infty} a_n \cos(\pi n\theta) + b_n \sin(\pi n\theta) \tag{6}$$

where  $a_n$  and  $b_n$  are the coefficients. The amplitude of the oscillations is calculated using Equation (2) and therefore the coil turns remain planar, which is required for making a valid Frenet-Serret frame without hard-way bending nor edge regression. Because the coefficients of the Fourier series are almost orthogonal it is simple to adjust the harmonics by hand. The  $a_1$  coefficient is the radius of the CCT layer:  $a_1 = 44$  mm for the inner layer and  $a_1 = 64$  mm for the outer layer. It is found that  $a_4 = 80 \mu\text{m}$  and  $a_6 = -15 \mu\text{m}$  used in both layers is sufficient to reduce all harmonics below 1 unit. The resulting harmonics tables computed by RAT are shown in Figure 3 to Figure 4. The reference radius used to calculate these harmonics was 20 mm.

harmonics given at a reference radius of: 20.000 [mm]

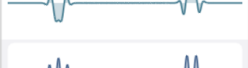
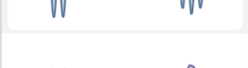
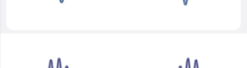
Order	An [T.m]	an	Normalized Shape	Order	Bn [T.m]	bn	Normalized Shape
A1	4.14e-05	0.12		B1	3.40e+00	10000.00	
A2	2.99e-05	0.09		B2	-1.93e-04	-0.57	
A3	1.31e-05	0.04		B3	1.70e-04	0.50	
A4	4.55e-06	0.01		B4	-5.32e-05	-0.16	
A5	2.07e-06	0.01		B5	-3.96e-05	-0.12	
A6	4.73e-07	0.00		B6	1.75e-06	0.01	
A7	3.48e-07	0.00		B7	6.73e-06	0.02	
A8	-2.70e-07	-0.00		B8	1.04e-08	0.00	
A9	5.55e-08	0.00		B9	-1.36e-07	-0.00	
A10	-3.93e-07	-0.00		B10	6.84e-09	0.00	

Figure 3. The integrated harmonic content of the two HTS tape design at a reference radius of 20mm.

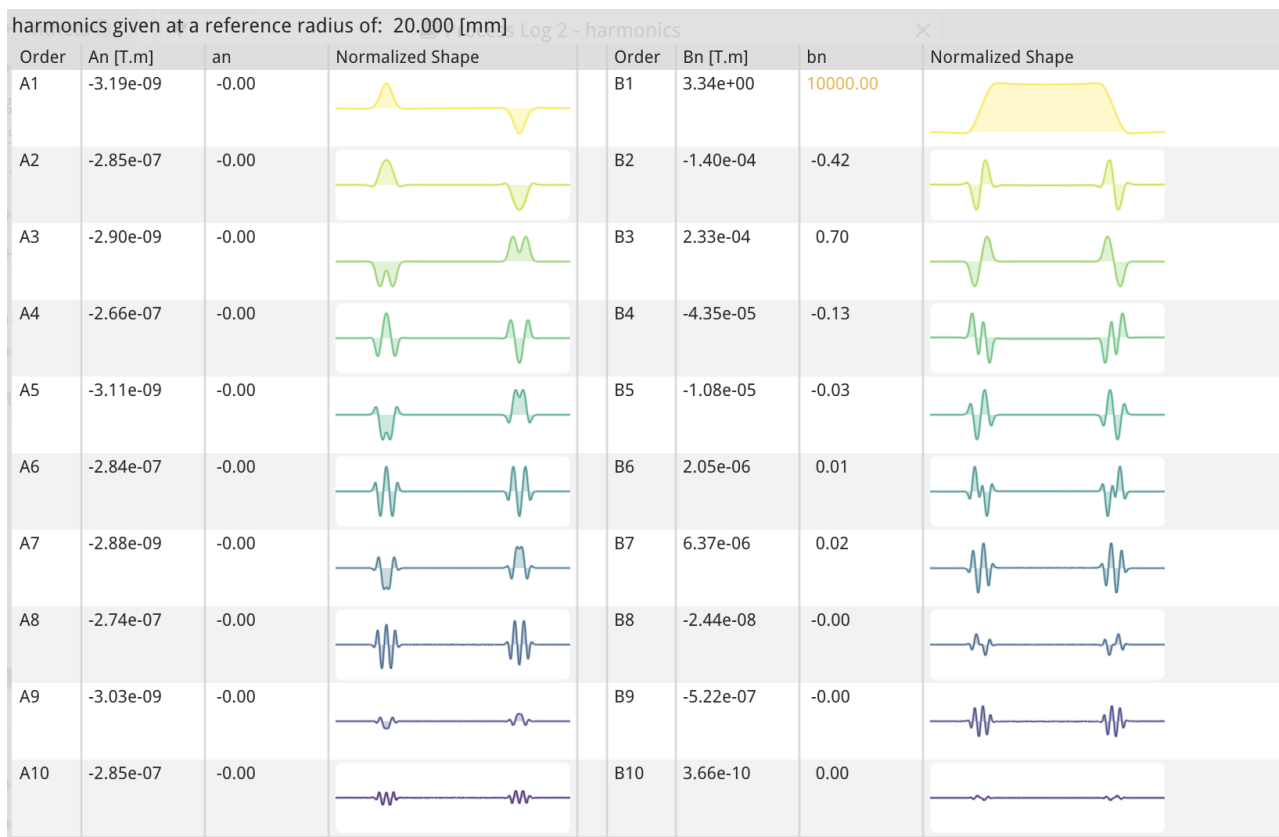


Figure 4. The integrated harmonic content of the four HTS tape design at a reference radius of 20mm.

Since the conductor is experiencing magnetic field at different angles (i.e., the tapes are not oriented with respect to B), a commonly adopted approach is to consider the critical current under transverse field for the sake of loadline margin. Considering Fujikura FESC-SCH04 [6], which has a 660 A at 20 K under 5 T transverse field, the resulting margin is 25%. This guarantees that, in the 4-tapes configuration, a local defect in one tape is not preventing operations near-to-nominal.

## 4. Materials and Manufacturing Concept

To avoid high shear stresses when winding the coil, the tapes inside the cable need to be soldered together after the winding process. The soldering can be performed by placing the whole coil in an oven. The maximum soldering temperature should be 200 °C [3]. Above this temperature there is a risk of degrading the HTS over time. The standard tin-lead solder melts around 180° C and has good electrical and mechanical properties. Low temperature solders could be considered but are usually more difficult to apply. The tapes can either be pre-tinned using electroplating, or some form of solder paste can be applied during winding, or in a solder bath that tapes pass through right before winding.

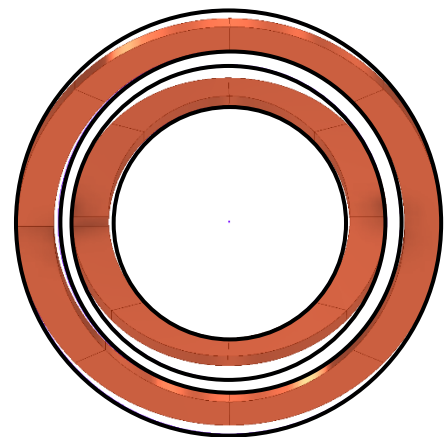
Bridging of the solder connecting one cable to the next in the same CCT slot is a major concern because it causes shorts. It is therefore proposed to perform the heat treatment separately for each cable, while each time applying stycast and polyimide between cables to create a boundary. The stycast will secure both the polyimide tape and the cables. Polyimide can be exposed to temperatures up to 260 °C [4], therefore it is suited to be used when the CCT goes in the oven for each soldering stage of the next cable. To ensure good electrical insulation the total thickness of the stycast and the polyimide layer is assumed to be around 200 µm.

Because the solder will melt every time the coil is placed in the oven, the cables need to stay under compression for as long as the CCT manufacturing process is underway. To this aim, a Teflon tube that fits in the CCT's slot can be pressed in the slot before the heat treatment to compress the tapes.

The manufacturing of this coil will be time consuming because of the winding process where each individual cable has to be soldered in an oven and then covered with insulation before the next cable can be wound in the same slot. This favours the four HTS tape design over the two-tape design.

To avoid shorting of the turns through the former (or shorts to ground) it should ideally be made of G11 or other insulating material if the mechanics allow it. However, if a metal former is unavoidable, it should be insulated before winding the conductor inside the slot. A possible solution for this could be an enamel-like coating of the former, for instance with Aremco SGC4000-HT [5]. This will ensure that the former is insulated from the conductor, and this glass insulation will be able to easily withstand the various soldering cycles in the oven.

Different former geometries are possible. This is due to the fact that the conductor is not describing circles in the cross-section plane (see scheme on the right, circles in purple). Therefore, it is possible to build a former which sustains only part, most, or all the conductor. For the sake of clearness, one of the possibilities is rendered in Figure 5. This option comes, of course, with a large material consumption and important voids to fill, so that a slimmer design should be investigated.



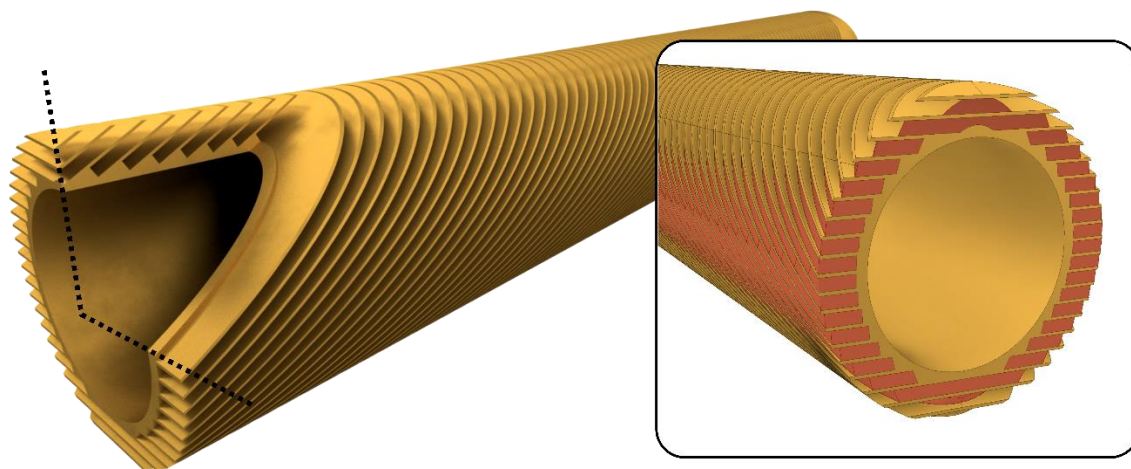


Figure 5. Conceptual geometry of the former for the inner layer, with cut views to highlight the shape. This concept is based on a “full supported cable” approach with round former, similar to cable based CCT with ribs. The ribs are 1 mm.

## 5. Thermal Design

Another requirement of the design is to have a fast-ramped magnet. Therefore, a minimum thermal margin is imposed on the design of the coil that is 10 K at an operating temperature of 20 K. This also affects the number of cables in a CCT slot: the higher the critical current of the HTS tapes, and the more HTS tapes per cable the higher the thermal margin. For the purpose of these studies, it was decided to use, again, the properties of Fujikura’s FESC-SCH04 tape [6]. This tape is characterized by measurement data. Current sharing is considered for the calculation of the temperature margin. This implies that the current can freely share across the width of the tape. Figures 6 shows the temperature margin in the coil for two and four tapes, respectively. The margin throughout the coil pack exceeds 10 K everywhere and is significantly larger in the majority of the coil.

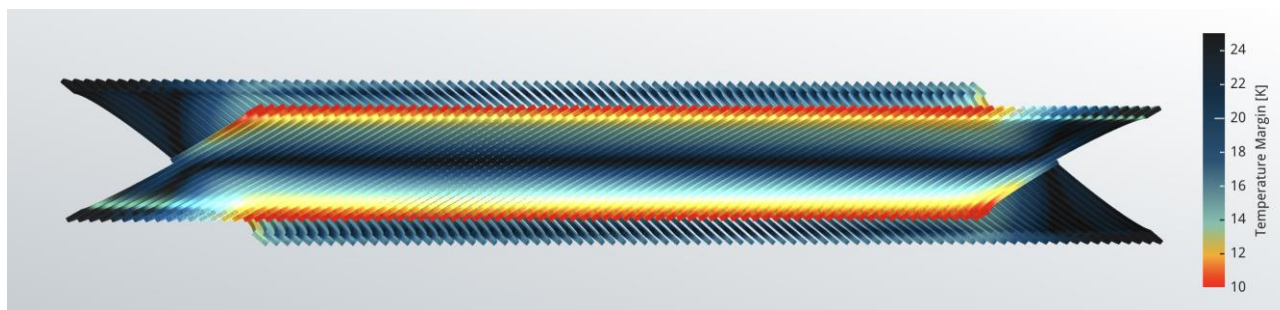


Figure 6a. Thermal margin of the two HTS tape design, clipped.

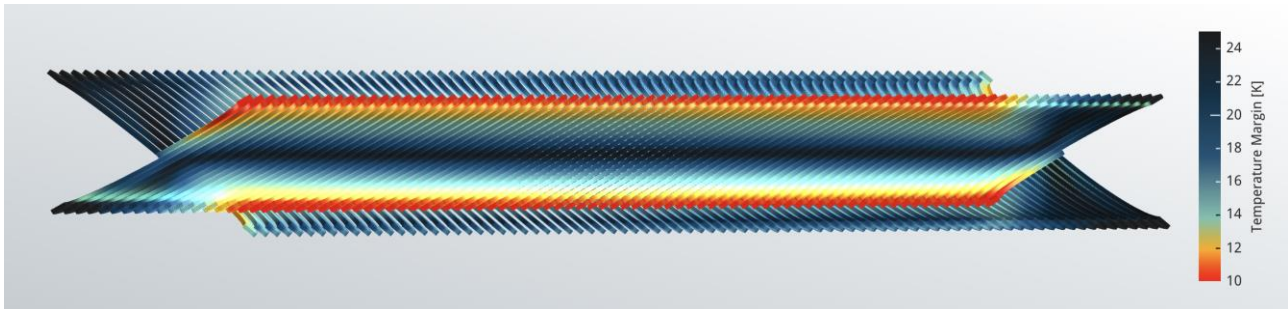


Figure 6b. Thermal margin of the four HTS tape design, clipped.

## 6. Quench Protection

To study the amount of copper stabilizer needed, first a two-dimensional adiabatic quench model was built with RAT and Raccoon, see Figure 7. A 200 mm long piece of all cables in a slot was modelled based on the cable shown in Figure 2 (this length is almost half turn, a length of CCT cable where uniform-field approximation is not unrealistic). For the stycast and polyimide insulation a thickness of 0.2 mm was chosen. The HTS tapes and the copper were modelled together in a current sharing model that is solved using the bi-section method. The HTS tapes were assumed to be Fujikura FESC-SCH04 and the copper stabilizer properties were chosen such that the copper RRR was 50.

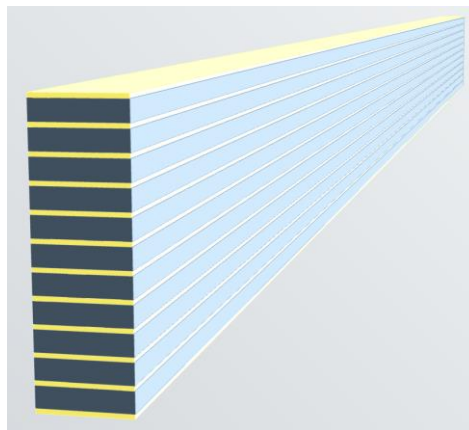


Figure 7. The two-dimensional piece of conductor for quench simulations.

A quench was started by simulating a spot heater at the edge of the cable stack, and the energy of the spot heater was chosen such that it was close to the minimum quench energy (MQE). The main purpose of the two-dimensional quench analysis was to determine the amount of copper needed for each cable as stabilizer and to redistribute the current after a quench. In addition, a scan of the quench detection voltage and a quench protection delay was performed.

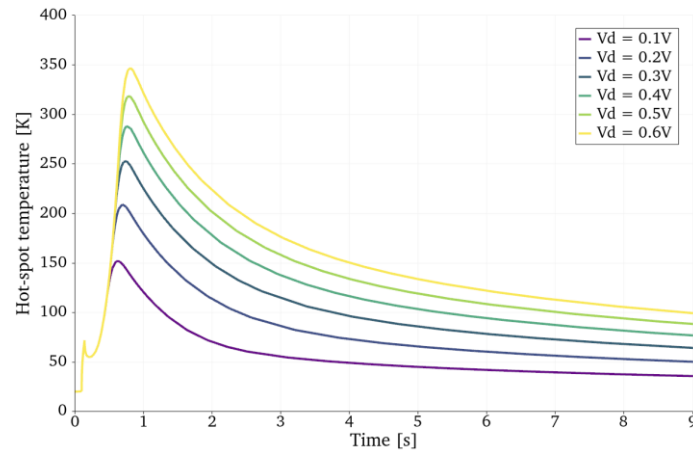
For quench detection it would be better to use a backing-wire that is co-wound with the CCT such that the inductive voltages can be subtracted from the quench voltage measurement that is used to

detect a quench. The voltages from AC-losses cannot be separated from the quench voltage measurement. Based on earlier work it is known that for the CCT demonstrator, which has two HTS tapes per cable, that is cycled from  $-4$  T to  $4$  T in  $20$  s the AC-losses are on average  $100$  W during cycling. For a coil that has an operating current of  $2000$  A this results in a voltage of  $0.05$  V, which is measured with the quench detection as well, and therefore the quench detection threshold should be well above this value. For the quench analysis used to study the copper thickness it was thus decided to use a voltage threshold of  $0.3$  V and a quench protection delay of  $0.02$  s. This protection delay can be achieved by using an IGBT switch that has a switching time in the order of  $5$  ms, short signal cables and a fast acquisition system.

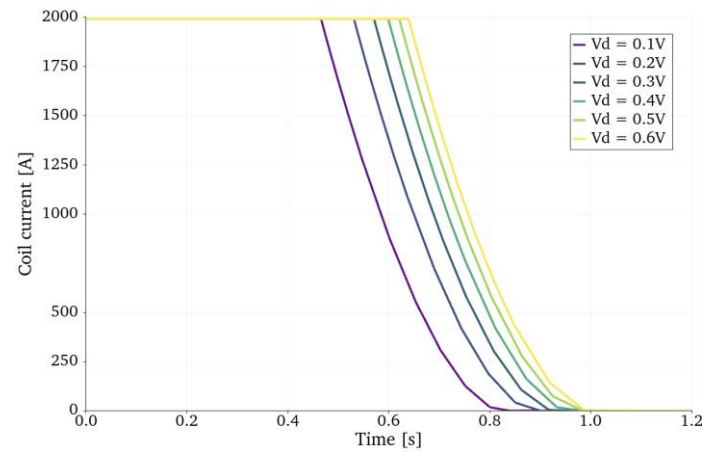
In all two-dimensional quench simulations described in this report the inductance of the coil ( $L = 240$  mH for two tapes,  $52$  mH for four tapes) is assumed to be connected in series with the quench propagation model. A transverse background field of  $4$  T is applied as well. The magneto resistance of the copper is also considered. Therefore, these two-dimensional simulations are representative for a quench happening in a critical location, where the peak field is at a right angle with respect to the tape. Other scenarios are to be investigated (such as the ones where the conductors surrounding the hot-spot have larger margin). Once a quench is detected in the simulation, meaning the voltage reached the voltage threshold chosen, and after the protection delay has passed, the power supply is switched off and simultaneously a Metrosil varistor unit is switched in series with the coil to extract the current as efficiently as possible [7]. The voltage over the Metrosil unit is given as  $V = C \cot I \beta$ , where  $I$  is the current,  $\beta$  a material property of the Metrosil in the order of  $0.42$  and  $C$  is a scaling factor calculated from the protection voltage. For these simulations, the protection voltage (voltage over the coil after the varistor switches in) was chosen to be  $500$  V.

Table 3 shows the hot-spot temperature versus the thickness of the copper stabilizer in a sub-layer for the case of two and four HTS tapes per sub-layer. As it can be expected, the more copper stabilizer, the lower the hot-spot temperature. For four HTS tapes per sub-layer the maximum hot-spot temperature is  $250$  K with  $700$   $\mu\text{m}$  of copper stabilizer, and for two tapes a similar hot-spot temperature can be found at  $350$   $\mu\text{m}$ . In general,  $250$  K is assumed to be a safe limit for the maximum hot-spot temperature of a HTS coil.

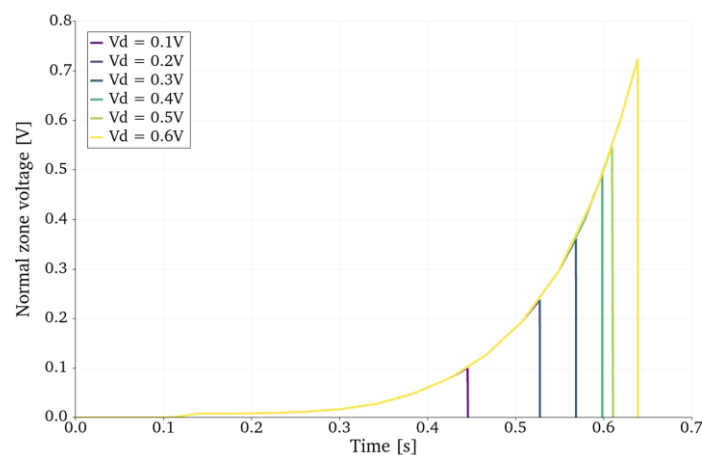
Next the two-dimensional simulation was used to study the quench detection threshold and protection delay. The effects of quench detection voltage threshold on the hot-spot temperature and current extraction are shown in Figure 8. For reference, the normal zone voltage is also shown in Figure 8c. It can be seen that after the voltage threshold is reached and the protection delay has passed, the protection switches on resulting in a current decay. According to the results shown in these plots, a protection voltage of  $0.3$  V is sufficient to protect the four tape CCT design. Based on the quench detection voltage of  $0.3$  V the effect of the quench protection delay is investigated. The resulting time transients are shown in Figure 9. Each time the protection delay is increased by  $0.01$  s the maximum hot-spot temperature increases by around  $12$  K.



(a) Hot-spot temperature.

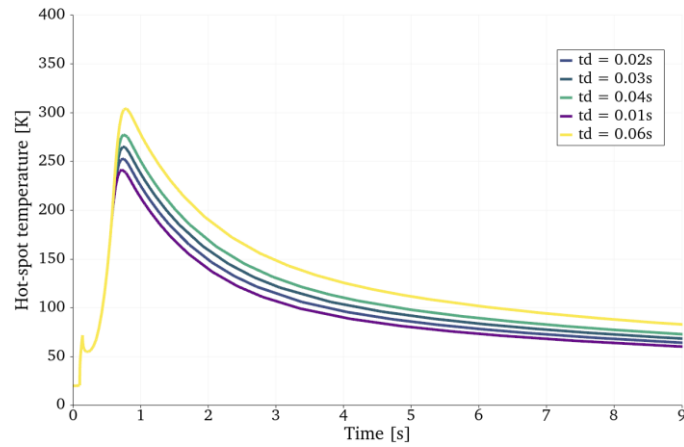


(b) Current in the coil.

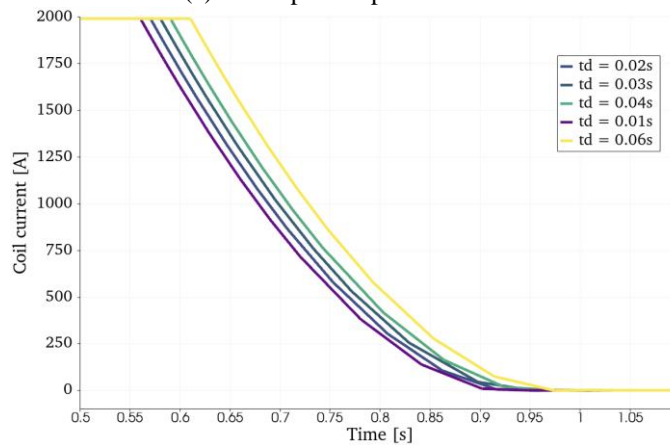


(c) The normal zone voltage.

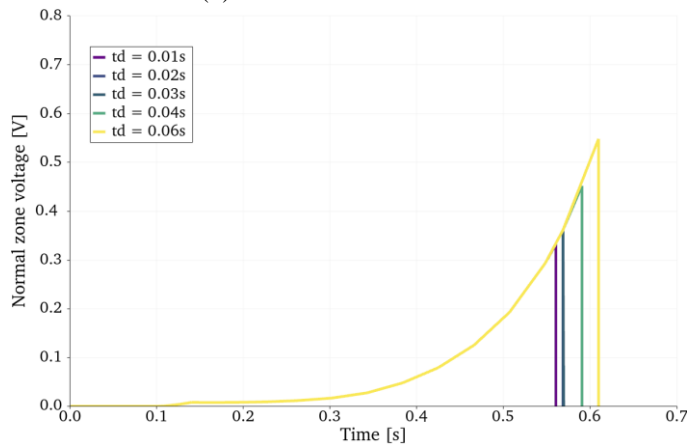
Figure 8. A two-dimensional quench simulation of a 200 mm long CCT layer with 11 sub-layers, four HTS tapes per sub-layer and 700  $\mu\text{m}$  copper stabilizer, for different quench detection voltages. During each simulation, the quench protection delay was set to be 0.02 s.



(a) Hot-spot temperature.



(b) Current in the coil.



(c) The normal zone voltage.

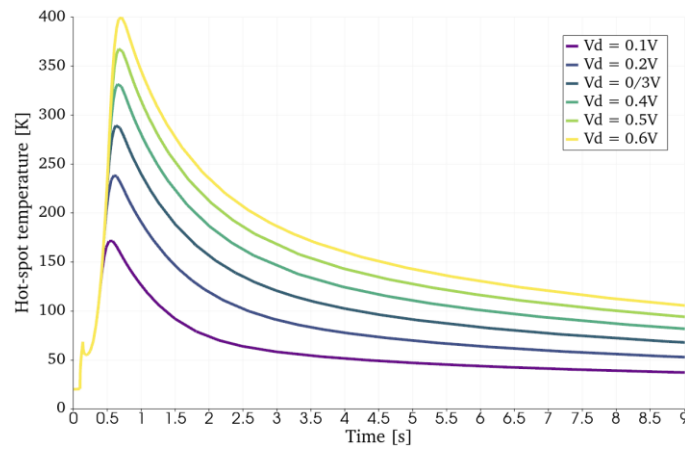
Figure 9. A two-dimensional quench simulation of a 200 mm long CCT layer with 11 sub-layers, four HTS tapes per sub-layer and 700  $\mu\text{m}$  copper stabilizer, for different quench protection delays. During each simulation, the quench detection voltage was set to be 0.3 V.

*Table 3: Hot-spot temperature versus copper stabilizer thickness.*

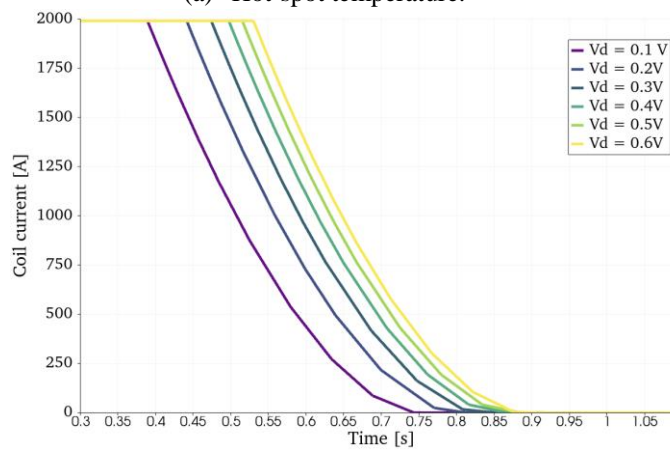
Thickness	Two HTS tapes		Four HTS tapes	
	Temperature [K]	MQE [J]	Temperature [K]	MQE [J]
350 $\mu\text{m}$	270	0.75		
400 $\mu\text{m}$			461	0.57
500 $\mu\text{m}$			348	0.66
600 $\mu\text{m}$			289	0.84
700 $\mu\text{m}$			252	1.05

For comparison the effects of the different quench protection voltage and time delay are also investigated for the four-tape case with only 600  $\mu\text{m}$  copper stabilizer per cable. As it can be seen from the results shown in Figure 10 one can also keep the maximum hot-spot temperature at around 250 K with 600  $\mu\text{m}$  stabilizer if one uses a voltage threshold of 0.2 V or less and a protection delay of 0.02 s. However, adding more copper stabilizer does not significantly affect the cost of this magnet while it does make protection easier.

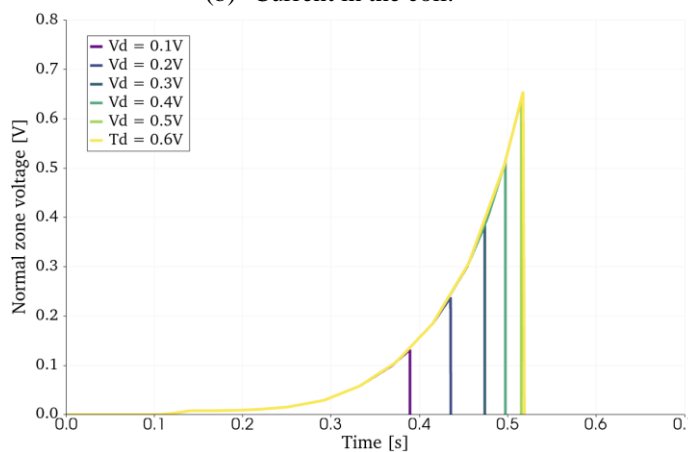
The influence of the protection delay on the quench behaviour for a two-dimensional CCT layer sample with 600  $\mu\text{m}$  copper stabilizer is shown in Figure 11. The maximum hot-spot temperature increases by around 15 K for each 0.01 s extra protection delay.



(a) Hot-spot temperature.

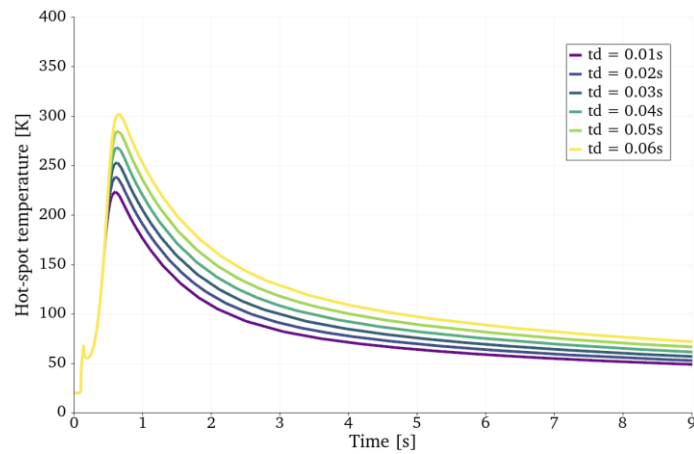


(b) Current in the coil.

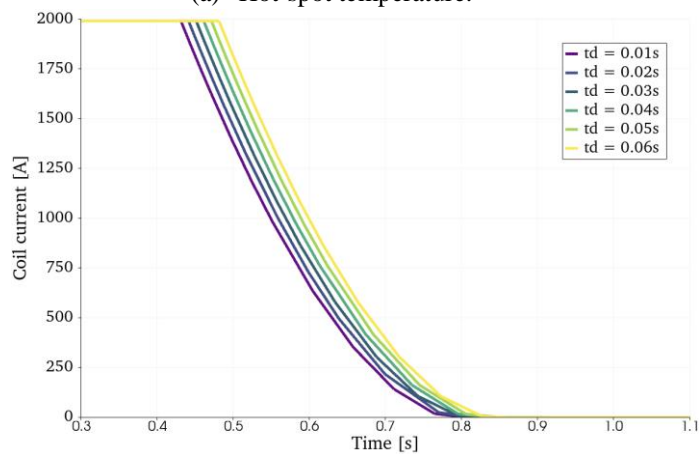


(c) The normal zone voltage.

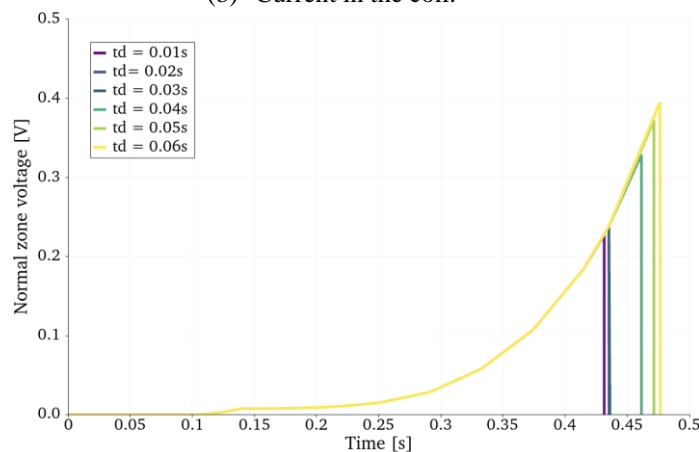
Figure 10. A two-dimensional quench simulation of a 200 mm long CCT layer with 11 sub-layers, four HTS tapes per sub-layer and 600  $\mu\text{m}$  copper stabilizer, for different quench detection voltages. During each simulation the quench protection delay was set to be 0.02 s.



(a) Hot-spot temperature.



(b) Current in the coil.



(c) The normal zone voltage.

Figure 11. A two-dimensional quench simulation of a 200 mm long CCT layer with 11 sub-layers, four HTS tapes per sub-layer and 600  $\mu\text{m}$  copper stabilizer, for different quench protection delays. During each simulation the quench detection voltage was set to be 0.2 V.

The CCT design with only two HTS tapes per cable was studied with a two-dimensional quench analysis. Based on the results from the four-layer case and the thermal margin requirement leading to 23 cables per slot and an operating current of 980 A it was decided to run the scans with 350  $\mu\text{m}$

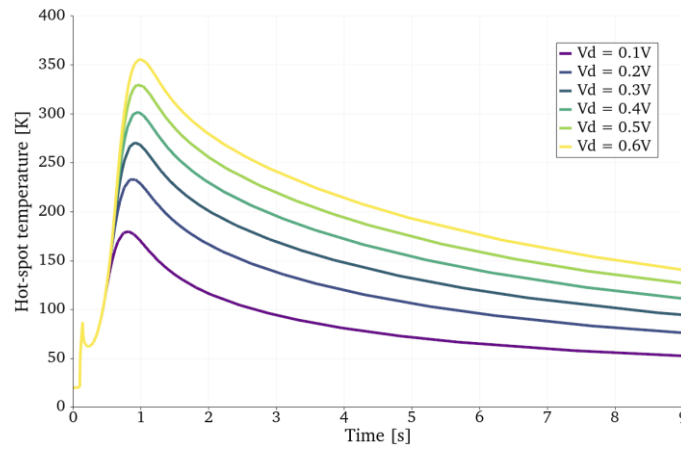
copper stabilizer only. Again, it was assumed that there was a perpendicular field of 4 T and the inductance of the CCT of 240 mH modelled to be in series with the 200 mm long cable section of CCT. The results of the voltage threshold scan can be found in Figure 12, and the quench protection delay scan is given in Figure 13. The hot-spot temperature is higher in this coil for the same quench detection settings. In case a two-HTS-tape coil would be preferential to a four-HTS-tape coil, it can be considered to use 400  $\mu\text{m}$  copper stabilizer per sub-layer to reduce the maximum hot-spot temperature after a quench. The results of the two-dimensional quench simulations are also summarized in Table 4 and Table 5 below.

*Table 4. Hot-spot temperature versus quench detection threshold for different copper stabilizer thicknesses. Each one-dimensional simulation had a protection delay of 0.02 s.*

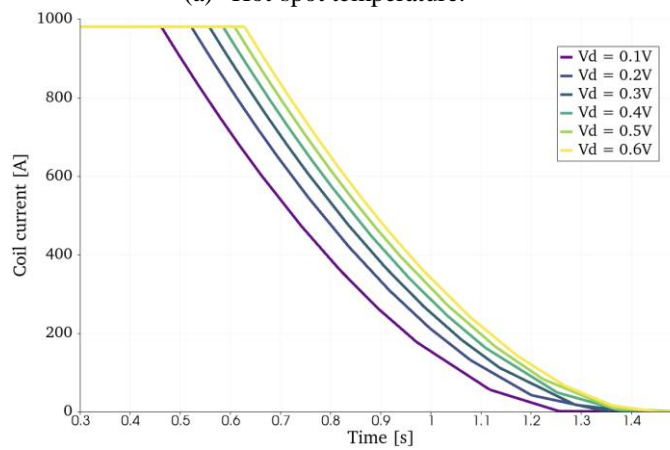
	Two HTS tapes	Four HTS tapes	
	350 $\mu\text{m}$	600 $\mu\text{m}$	700 $\mu\text{m}$
$V_d$ [V]	$T_{\text{hot-spot}}$ [K]	$T_{\text{hot-spot}}$ [K]	$T_{\text{hot-spot}}$ [K]
0.1	180	171	151
0.2	235	238	210
0.3	270	289	252
0.4	301	331	287
0.5	330	367	317
0.6	356	397	344

*Table 5. Hot-spot temperature versus quench detection threshold for different copper stabilizer thicknesses. The voltage threshold used during each scan is giving in the table.*

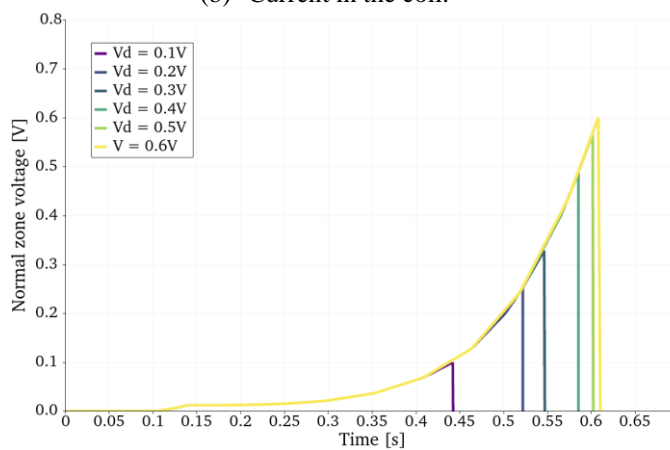
	Two HTS tapes	Four HTS tapes	
	350 $\mu\text{m}$	600 $\mu\text{m}$	700 $\mu\text{m}$
$V_{\text{Th}}$	0.2 V	0.2 V	0.3 V
$t_d$ [s]	$T_{\text{hot-spot}}$ [K]	$T_{\text{hot-spot}}$ [K]	$T_{\text{hot-spot}}$ [K]
0.01	224	224	241
0.02	235	238	252
0.03	242	252	264
0.04	253	268	277
0.05	263	284	290
0.06	275	302	304



(a) Hot-spot temperature.

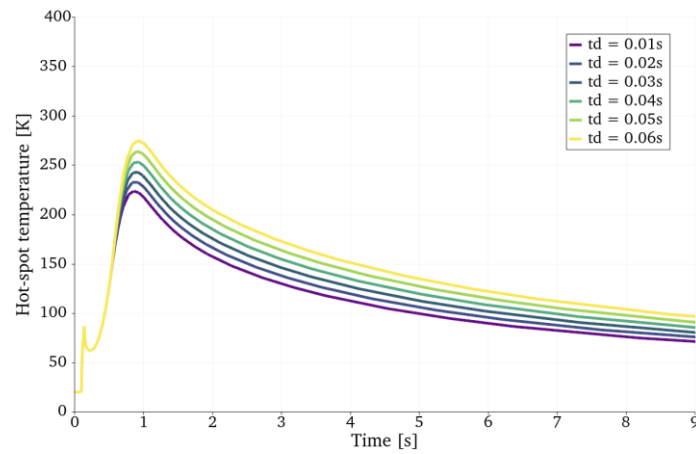


(b) Current in the coil.

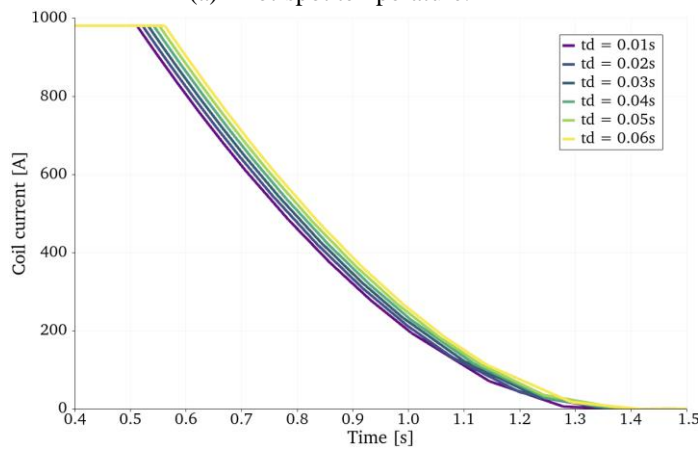


(c) The normal zone voltage.

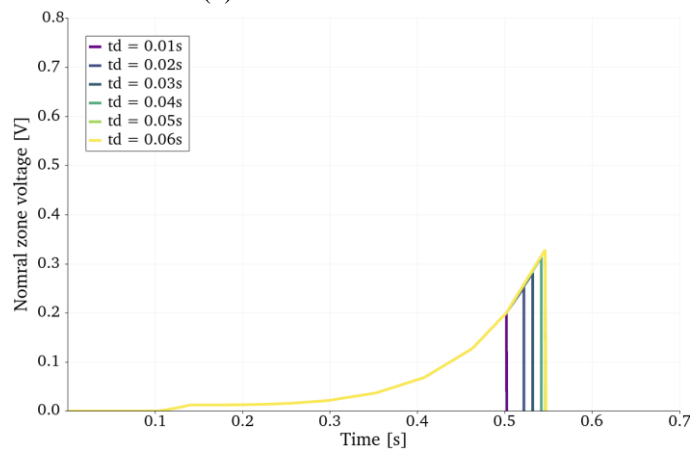
Figure 12. two-dimensional quench simulation of a 200mm long CCT layer with 11 sub-layers, two HTS tapes per sub-layer and 350  $\mu\text{m}$  copper stabilizer, for different quench detection voltages. During each simulation the quench protection delay was set to be 0.02 s.



(a) Hot-spot temperature.



(b) Current in the coil.



(c) The normal zone voltage.

Figure 13. A two-dimensional quench simulation of a 200 mm long CCT layer with 11 sub-layers, two HTS tapes per sub-layer and 350  $\mu\text{m}$  copper stabilizer, for different quench protection delays. During each simulation the quench detection voltage was set to be 0.2 V.

## 7. AC losses and Dynamic Field Quality

To determine if two or four tapes should be used in this CCT design the AC-losses during ramping were evaluated. This magnet will be ramped from 0 T to 4 T in under 10 s, and during this ramp screening currents in the HTS tapes cause for AC-losses. It is important that the cooling is able to provide enough cooling power to deal with these losses.

A Raccoon [2] model was created to simulate AC-losses in the coil when ramping the coil to 4 T in 10 s, then maintaining the operating current for another 10 s and ramp it back down to 0 T, again in 10 s. In this model, each tape was simulated separately. This means that the calculation time for a full-scale, 84 turn coil would be too long, and therefore only 22 were simulated, and then the AC-losses from the 22 turn model were scaled to obtain the AC-losses for the full scale coil.

In Raccoon the AC-losses were calculated as  $P_{AC} = \vec{j} \cdot \vec{E}_R$ , where  $P_{AC}$  is the AC-loss power,  $\vec{j}$  the current density and  $\vec{E}_R$ , the resistive part of the electric field  $\vec{E}$ , which is equal to  $\vec{E} = \vec{E}_R + \vec{E}_I$ . The inductive part of the electric field is not used in the AC loss calculation because that is converted to the stored magnetic energy during ramping. The current profile for the AC-loss calculation is shown in Figure 14. For both the two and the four-tape case the current is cycled between 0 T and 4 T two times.

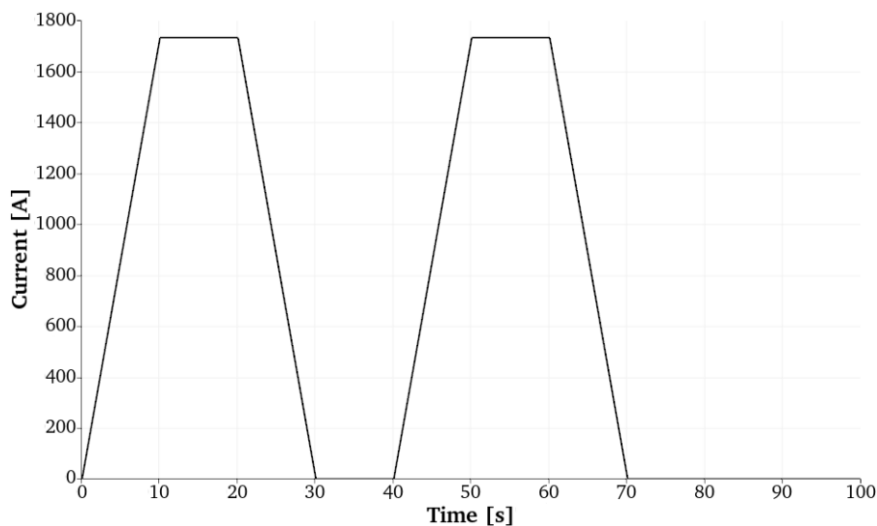


Figure 14. The current profile during the ramping of a sub-scale model for the AC-loss calculations. The current is cycled two times for both the two and the four-tape case.

The resulting AC-losses versus time for both designs are shown in Figure 15. The first peak in the plot is from the virgin ramp and the three peaks after are the first ramp down, the second ramp up and the second ramp down respectively. The AC-losses in both designs have a peak at 140W during a ramp. The average is 50 watts, which can be cooled with cryocoolers. The peak value can be smeared

out in time by the heat capacity of the system. If the heat capacity of the system is not sufficient then additional heat capacity can be added in the form of a copper block.

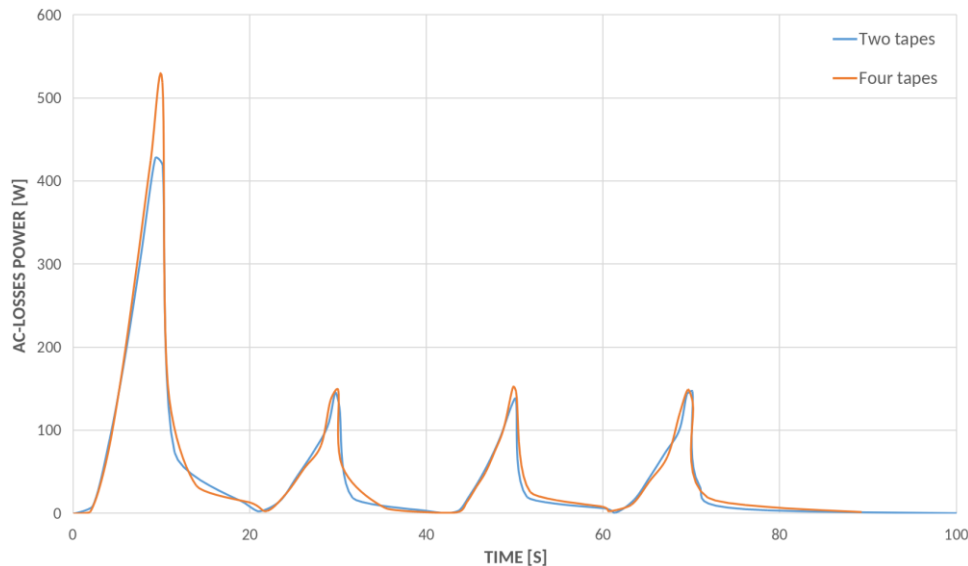


Figure 15. The AC-losses in the two tape (blue) and the four tape (orange) design of the HTS CCT demonstrator.

Even though on design it has two times the amount of HTS tapes in a slot, in the two tape design each slot has double the amount of cables and therefore the AC-losses are comparable for both designs. The net number of tapes in a CCT slot are the same for both designs, the difference is the amount of insulation between the tapes.

The results in Figure 15 suggest that the AC-losses in this design are dominated by the hysteresis losses. The current density in the cross-section of the 22 turn IFAST CCT model with four tapes at  $t = 45$  s of the simulation is shown in Figure 16.

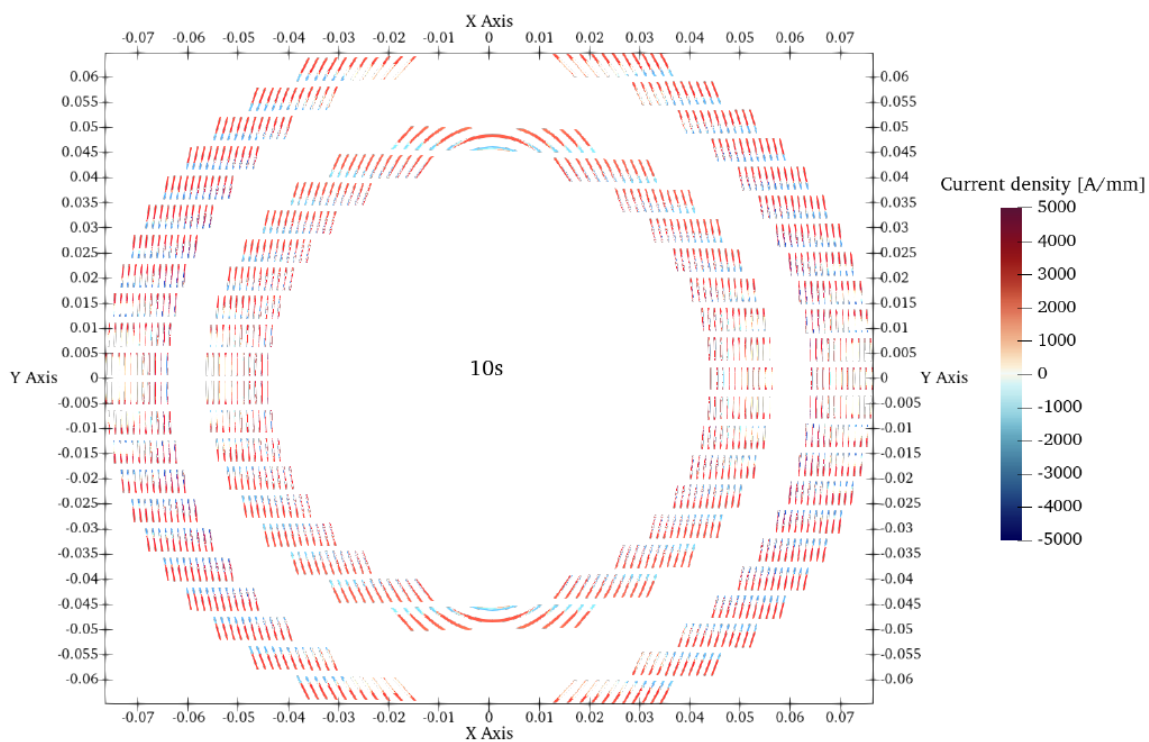


Figure 16. The current density in the four-tape design of the IFAST CCT at 10 s, at the end of the first ramp up.

---

## 8. Conclusions

---

The HTS demonstrator magnet was designed using a CCT layout. Due to the flat REBCO HTS tapes, hard-way bending must be avoided or minimized. It was shown that this can be achieved using a Frenet-Serret frame on the CCT equations.

Based on this layout, this report proposed two geometries for the 4 T magnet demonstrator: 1) a CCT with a cable with two tapes with a width of 4mm and 23 cables in each slot of the two formers, with an operating current of 970 A; and 2) a CCT with a cable that has four tapes with a width of 4mm and 11 cables in each slot of the two formers. It has an operating current of 1990 A.

Assuming FESC tape from Fujikura, both designs have a temperature margin of 10 K at an operating temperature of 20 K. The AC-losses for both the two-tape and the four-tape design are on average 50 W during operation. This opens the possibility of a two-cryocoolers system. Loadline margin is about 25%, favouring the 4 tapes configuration for the sake of safeness and stability.

The tapes, both the HTS and the copper stabilizer tapes, should be soldered together in the cable to improve current sharing. Due to bending shear stress, it is not possible to solder the cable before coil winding. It will be necessary to wind the coil from separate spools and tensioners and solder the tapes together into a cable after the tapes are wound individually onto the former.

An adiabatic quench analysis was used to determine the required thickness of copper stabilizer tapes in the cable. For a quench detection voltage threshold of 0.3 V, a protection delay of 20 ms and a protection voltage of 500 V using Metrosil, it was computed that 350  $\mu\text{m}$  and 700  $\mu\text{m}$  of copper is needed for the two and four tape designs respectively, to keep the peak temperature below an acceptable 250 K. Feasibility and practical aspects in magnet fabrication are going to lead the choice between two and four tapes, as far as on paper both solutions work.

The next steps involve defining the formers for the coil, which will likely be made of Aluminum-Bronze, and determining the winding procedure using either two or four tape cables. The mechanical components will be verified using FEM simulations. Another area of focus is the splice/joints of the cables, which will undergo experimental testing with different concepts.

## Acknowledgements

IFAST WP8 group thanks Jeroen van Nugteren and Little Beast Engineering for their support in computations and developments for the magnet presented in this document.

## References

- [1] Russenschuck, S. (2011). Field computation for accelerator magnets: analytical and numerical methods for electromagnetic design and optimization. John Wiley & Sons
- [2] <https://www.littlebeastengineering.com/>
- [3] Lu, J., Xin, Y., Javis, B. & Bai, H. Oxygen out-diffusion in REBCO coated conductor due to heating (2021).
- [4] 3M Science Applied to Life. 3M™ Polyimide Film Tape 5413  
<https://multimedia.3m.com/mws/media/1360110/3m-polyimide-film-tape-5413-tds.pdf>.
- [5] Aremco Products, Inc. High Temperature Electrical Coatings and Sealants  
[https://aremco.com/wp-content/uploads/2020/07/A05\\_S1\\_Electrical\\_20.pdf](https://aremco.com/wp-content/uploads/2020/07/A05_S1_Electrical_20.pdf).
- [6] Superconductor Business Development Division, Fujikura Ltd. Introduction of Fujikura RE-based High-Temperature Superconductor  
<https://www.fujikura.co.jp/eng/products/newbusiness/superconductors/01/superconductor.pdf>
- [7] M and I Materials. SUPERCONDUCTING QUENCH PROTECTION  
<https://metrosil.com/wp-content/uploads/2021/09/Quench-Protection-with-Metrosil.pdf>.